UNIVERSITY OF BIRMINGHAM | COLLEGE OF ENGINEERING AND PHYSICAL SCIENCES

Nonlinear Analysis to Quantify Movement Variability in Human-Humanoid Interaction

Presentation of my PhD VIVA

Birmingham, UK, 11 January 2019

PhD Student: Miguel Xochicale

Primary supervisor: Chris Baber. **Secondary Supervisor:** Martin Russell

External Examiner: Max A. Little. **Internal Examiner:** Tim J. Jackson

School of Engineering
University of Birmingham, UK

Overview of the PhD thesis

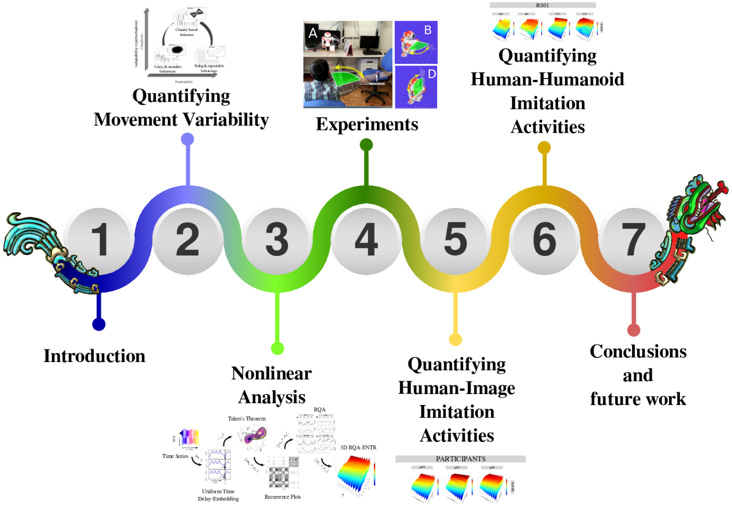

(Xochicale 2019 in **PhD thesis**)

MOVEMENT VARIABILITY

Why is challenging to investigate Human Movement Variability?

Human movement variability not only involves multiple joints and limbs for a specific task in a determined environment but also
external information processed through:
* all of our available senses and
* our prior experiences.

(Xochicale 2019 in **PhD thesis**)

Modelling Movement Variability

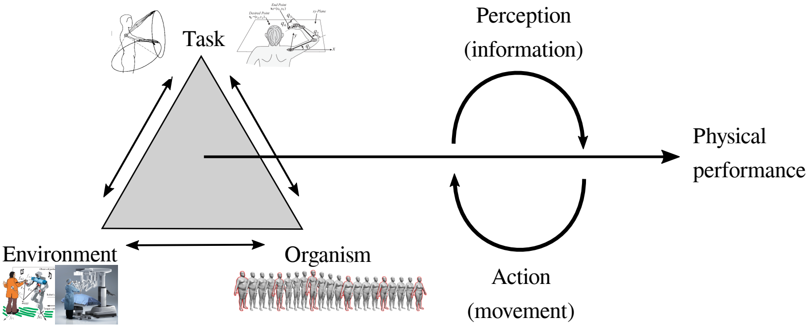

Figure 1: Newell's model of movement constrains

(Bernstein 1967 in **The co-ordination and regulation of movements**; Newell and Vaillancourt 2001 in **Hum Mov Sci**; Davids et al. 2003 in **Sport Medicine**)

Modelling Movement Variability

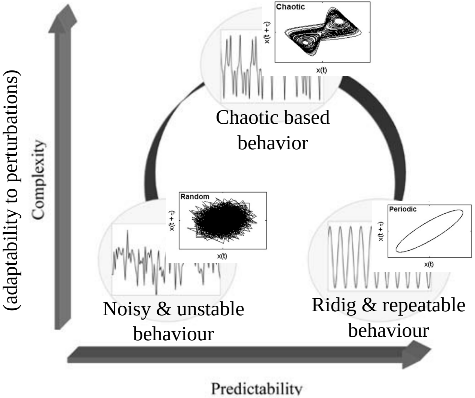

Figure 2: Theoretical Model of Optimal Movement Variability

(Stergiou et al. 2006 in **Neurologic Physical Therapy** Stergiou and Decker 2011 in **Human Movement Science**)

Nonlinear Analysis

- Reconstructed State Space (Takens 1981)
- Recurrence Plots (Eckmann et al. 1987, Marwan et al. 2007)
- Approximate Entropy (Pincus 1991, 1995)
- Sample Entropy (Richman and Moorman, 2000)
- Largest Lyapunov exponent (Stergiou, 2016)
- Recurrence Quantification Analysis (Zbilut and Webber et al., 1992)

There is no best tool to quantify MV and unification of tools is still an open question (Caballero et al. 2014; Wijnants et al. 2009) which led me (i) to explore different nonlinear analysis to measure MV and (ii) to understand their strengths and weaknesses.

(Caballero et al. 2014 in **European Journal of Human Movement**; Wijnants et al. 2009 in **Nonlinear Dynamics, Psychology, and Life Sciences**)

Research Questions

- What are the effects on RSSs, RPs, and RQA metrics of different embedding parameters, different recurrence thresholds and different characteristics of time series (structure, smoothness and window length size)?
- What are the weaknesses and strengths of RQA metrics when quantifying movement variability?
- How does the smoothing of raw time series affect methods of nonlinear analysis when quantifying movement variability?

(Xochicale 2019 in **PhD thesis**)

NONLINEAR ANALYSIS

State Space Reconstruction Theorem

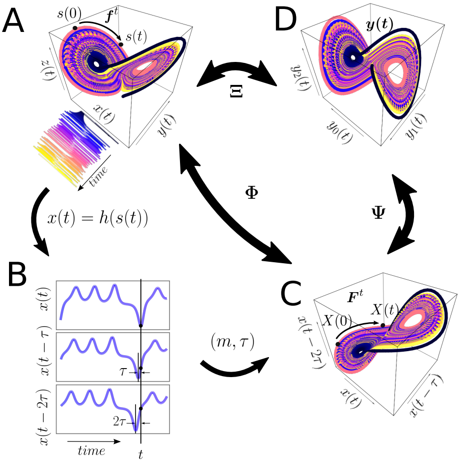

Figure is adapted from (Casdagli et al. 1991; Quintana-Duque (2012); Uzal et al. 2011)

(Takens F 1981 in **Dynamical Systems and Turbulence**; Casdagli 1991 in **Physica D**)

Takens's Theorem

$$s(t) = f^t[s(0)]$$

- s represents a trajectory which evolves in an unknown $d-$dimensional manifold M
- f^t is a evolution function with time evolution t

Then

$$x(t) = h[s(t)]$$

- $x(t)$ scalar time series in $\mathbb{R}$
- h is a function defined on the trajectory $s(t)$

(Takens F 1981 in **Dynamical Systems and Turbulence**; Casdagli 1991 in **Physica D**)

State Space Reconstruction Theorem

Uniform time-delay embedding matrix
$X(t) = \{x(t), x(t-\tau), ..., x(t-(m-1)\tau)\}$ defines a map
$\Phi : M \to \mathbb{R}^m$ such that

$$X(t) = \Phi(s(t))$$

where Φ is a diffeomorphic map whenever $\tau > 0$ and $m > 2d_{box}$
and d_{box} is the box-counting dimension of M.

(Takens F 1981 in **Dynamical Systems and Turbulence**; Casdagli 1991 in **Physica D**)

Uniform Time-Delay Embedding (UTDE)

For a given discrete time series $\{x_n\}_{n=1}^{N} = [x_1, x_2, \dots, x_N]$ of sample length N, a uniform time-delay embedding matrix is defined as

$$\mathbf{X}_{\tau}^{m} = \begin{pmatrix} \tilde{x}_n \\ \tilde{x}_{n-\tau} \\ \vdots \\ \tilde{x}_{n-(m-1)\tau} \end{pmatrix}^{T}$$

where m is the **embedding dimension** and τ is the **embedding delay**.

The sample length for $\tilde{x}(n - i\tau)$, where $0 \leq i \leq (m-1)$, is $N - (m-1)\tau$, and the dimensions of $\mathbf{X}_{\tau}^{m}$ are $(m, (N-(m-1)\tau))$.

(Frank et al. 2010 in **AAAI Conference on Artificial Intelligence** and Sama et al. 2013 in **Neurocomputing**)

Estimation of Embedding Parameters

False Nearest Neighbours (FNN) for m

Unfold the attractor (i.e. evolving trajectories in a state space).

Average Mutual Information (AMI) for τ

Maximize the information in the RSSs.

(Cao L. 1997 in **Physica D**; Kabiraj et al. 2012 in **Chaos**)

False Nearest Neighbours (FNN) for embedding dimension

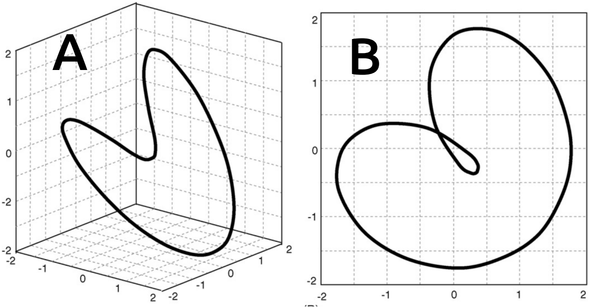

Figure 2 England 2007.

Figure 3: (A) Plot of $x(t) = \sin(2\pi t) + \cos(2\pi t)$ with embedding dimension $n = 3$ and (B) $n = 2$. Note that the false-nearest-neighbor illustrated by the intersectoin (-0.25, 0.25) when $n = 2$.

False Nearest Neighbours (FNN) for embedding dimension

False Nearest Neighbours (FNN)

$$E(m) = \frac{1}{N - m\tau} \sum_{i=1}^{N-m\tau} \frac{||X_i(m+1) - X_{n(i,m)}(m+1)||}{||X_i(m) - X_{n(i,m)}(m)||}$$

$E_1(m)$ and $E_2(m)$

$$E_1(m) = \frac{E(m+1)}{E(m)} \quad E_2(m) = \frac{E^*(m+1)}{E^*(m)}$$

(Cao L. 1997 in **Physica D**)

False Nearest Neighbours (FNN) for embedding dimension

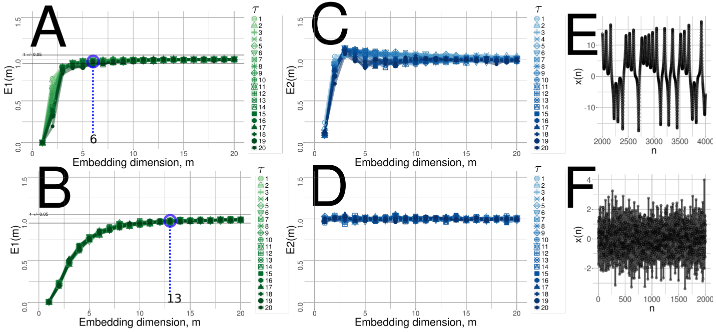

Figure is adapted from Cao L 1997 in **Physica D**

Figure 4: (A,B) $E_1(m)$ and (C, D) $E_2(m)$ values for (E) chaotic and (F) random time series

Average Mutual Information (AMI) for embedding delay

In order to obtain τ_0, "it has to be found in the first minimum of $I(\tau)$ where $x(n+\tau)$ adds maximal information to the knowledge from $x(n)$" meaning that the redundancy between $x(n+\tau)$ and $x(n)$ is the least .

(Kantz et al. 2003 in **BOOK: Nonlinear Time Series Analysis**)

Average Mutual Information (AMI) for embedding delay

Average Mutual Information (AMI)

$$I(\tau) = \sum_{i,j}^{N} p_{ij} log_2 \frac{p_{ij}}{p_i p_j}.$$

where: p_i is the probability that $x(n)$ has a value inside the i-th bin of the histogram, p_j is the probability that $x(n+\tau)$ has a value inside the j-th bin of the histogram and $p_{ij}(\tau)$ is the probability that $x(n)$ is in bin i and $x(n+\tau)$ is in bin j.

(Kabiraj et al. 2012 in **Chaos**)

Average Mutual Information (AMI) for embedding delay

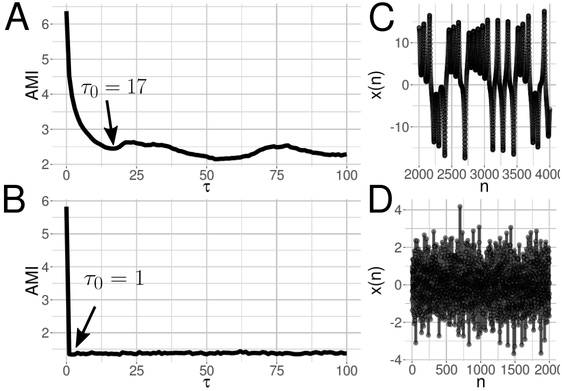

Figure is adapted from Kabiraj et al. 2012 in **Chaos**

Figure 5: (A, B) AMI values for (C) chaotic and (D) noise time series.

Recurrence Plot (RP)

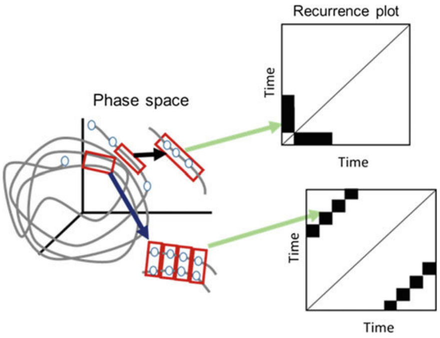

Figure is from Pawar 2018.

Figure 6: The vertical lines in the RP show that more that one point of the same trajectory are recurring at the same time. The diagonal lines in the RP depict that two trajectories are running in parallel to each other.

(Pawar et al. 2018)

Recurrence Plot

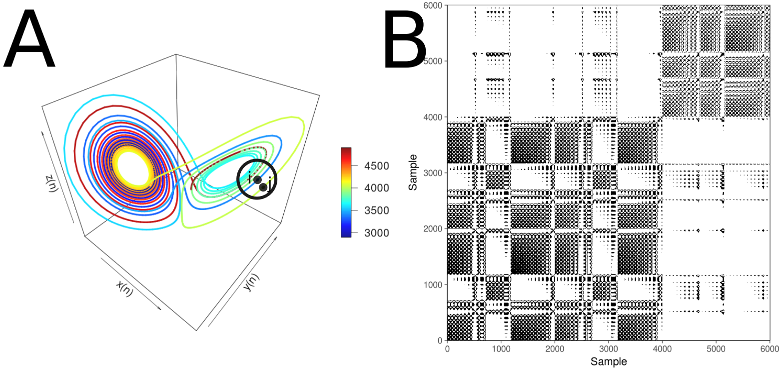

Figure is adapted from (Marwan et al. 2007)

Figure 7: (A) State space for Lorenz systems, and (B) Recurrence plot with embeddings ($m = 1$, $\tau = 1$) and $\epsilon = 5$

Recurrence Plots

$\mathbf{R}^{m}_{i,j}(\epsilon)$ is two dimensional plot of $N \times N$ square matrix defined by

$$\mathbf{R}^{m}_{i,j}(\epsilon) = \Theta(\epsilon_i - \|X(i) - X(j)\|), \quad i, j = 1, \dots, N$$

where N is the number of considered reconstructed states of $X(i)$ ($X(i) \in \mathbb{R}^m$), ϵ is a threshold distance, $\| \cdot \|$ a norm, and $\Theta(\cdot)$ is the Heaviside function.

(Eckmann et al. 1987 in **Europhysics Letters**)

Recurrence Plot Patterns

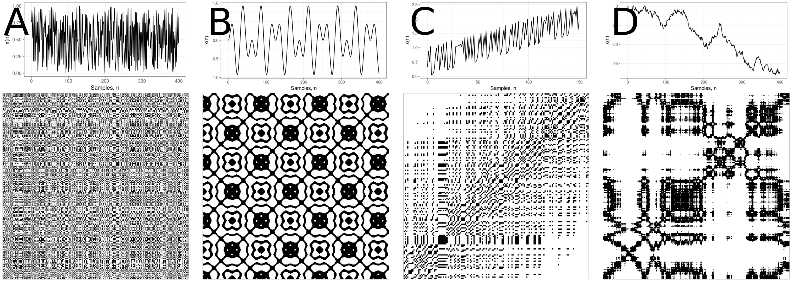

Figure is adapted from (Marwan et al. 2007)

Figure 8: Recurrence plots for (A) uniformly distributed noise, (B) super-positionet harmonic oscillation, (C) drift logistic map with a linear increase term, and (D) disrupted brownian motion.

Recurrence Quantification Analysis (RQA)

REC enumerates the black dots in the RP.

$$REC(\epsilon, N) = \frac{1}{N^2 - N} \sum_{i \neq j = 1}^{N} \mathbf{R}_{i,j}^{m}(\epsilon)$$

DET fraction of recurrence points that form diagonal lines. *(interpreted as the predictability where, for example, periodic signals show longer diagonal lines than chaotic ones.)*

$$DET = \frac{\sum_{l=d_{min}}^{N} lH_D l}{\sum_{i,j=1}^{N} \mathbf{R}_{i,j}^{m}(\epsilon)}$$

(Marwan and Webber, 2015)

Recurrence Quantification Analysis (RQA)

RATIO is the ratio of DET to REC. *(useful to discover dynamic transitions)*.

ENTR Shannon entropy of the frequency distribution of the diagonal line lengths. *(useful to represent the complexity of the structure of the time series)*

$$ENT = -\sum_{l=d_{min}}^{N} p(l) ln p(l),$$

where

$$p(l) = \frac{H_D(l)}{\sum_{l=d_{min}}^{N} H_D(l)}$$

(Marwan and Webber, 2015)

RQA

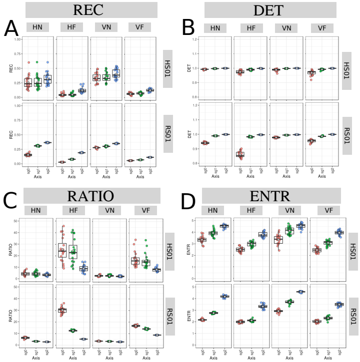

Figure is adapted from Xochicale 2019

Figure 9: Recurrence Quantification Analysis with $m_0 = 6$, $\tau_0 = 8$ and $\epsilon = 1$.

3D surface plots of RQA

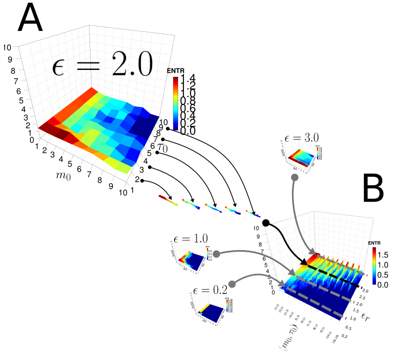

Figure is adapted from Xochicale 2019

Figure 10: (A) 3D surface plots for with increasing pair of embedding parameters ($0 \leq m \leq 10$, $0 \leq \tau \leq 10$) and $\epsilon = 3.0$. (B) Surface plot A with decimal increase of 0.1 for recurrence thresholds ($0.2 \geq \epsilon \leq 3$).

(Xochicale 2019 in **PhD thesis**)

3D surface plots of RQA

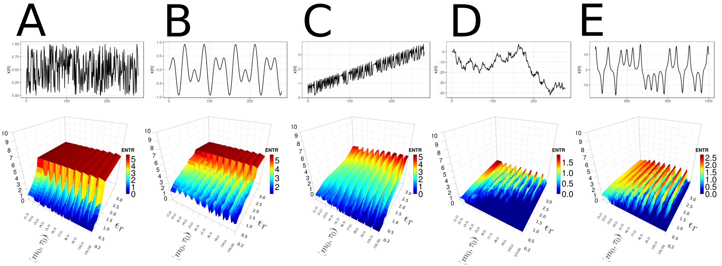

Figure is adapted from Xochicale 2019

Figure 11: 3D surface plots for (A) uniformly distributed noise, (B) super-positionet harmonic oscillation, (C) drift logistic map with a linear increase term, (D) disrupted brownian motion, and (E) Lorenz system.

EXPERIMENT

Participants

Originally, 23 right-handed healthy participants were invited for two experiments, however some of these were not considered in the analysis due to technical problems with IMU's.

Human-Image Imitation Activity

6 participants ($p01, p04, p05, p10, p11, p15$) with mean and standard deviation (SD) age of mean=19.5 (SD=0.83) years.

Human-Humanoid Imitation Activity

20 participants with mean and standard deviation (SD) age of mean=19.8 (SD=1.39) years, being four females and sixteen males.

(Xochicale 2019 in **PhD thesis**)

Human-Image Imitation Activities

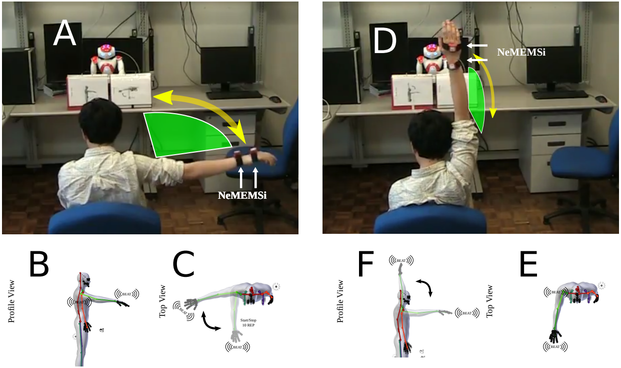

Figure 12: Human-Image Imitation Activities of Arm Movements for two speed conditions: Horizontal Normal (HN) and Horizontal Faster (HF).

(Xochicale 2019 in **PhD thesis**)

Human-Humanoid Imitation Activities

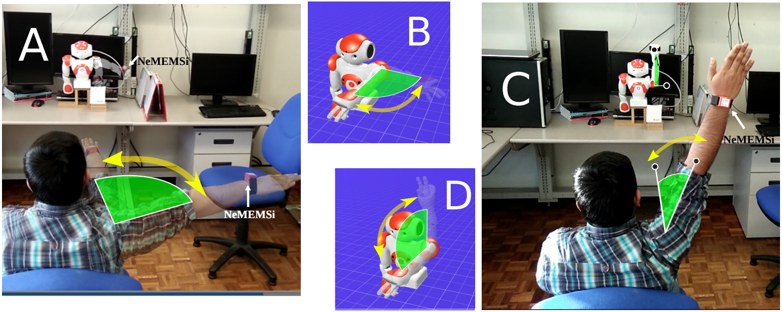

Figure 13: (A/C) Front-to-Front Human-Humanoid Imitation Activities of Horizontal/Vertical Movements, (B/D) NAO, humanoid robot, performing Horizontal/Vertical arm movements.

RESULTS

From Raw to Smoothed Time Series

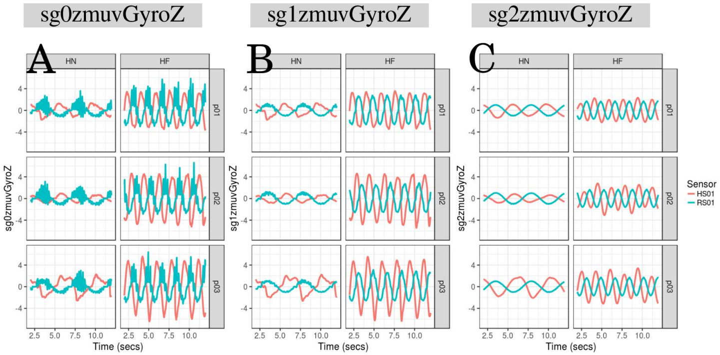

Figure 14: Time-series of horizontal movements for (A) normalised, (B) sgolay(p=5,n=25), and (C) sgolay(p=5,n=159).

(Xochicale 2019 in **PhD Thesis**)

From Raw to Smoothed Time Series

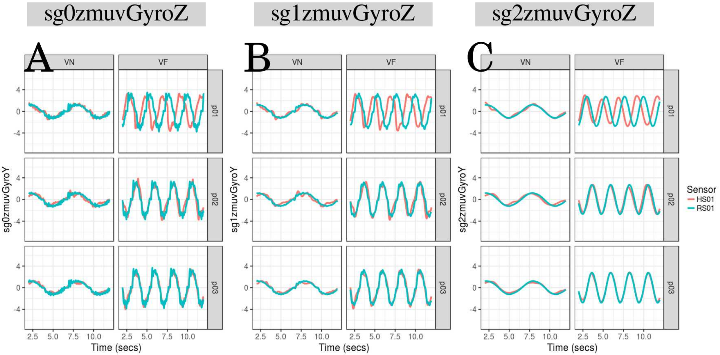

Figure 15: Time-series of vertical movements for (A) normalised, (B) sgolay(p=5,n=25), and (C) sgolay(p=5,n=159).

(Xochicale 2019 in **PhD Thesis**)

Minimum Embedding Parameters

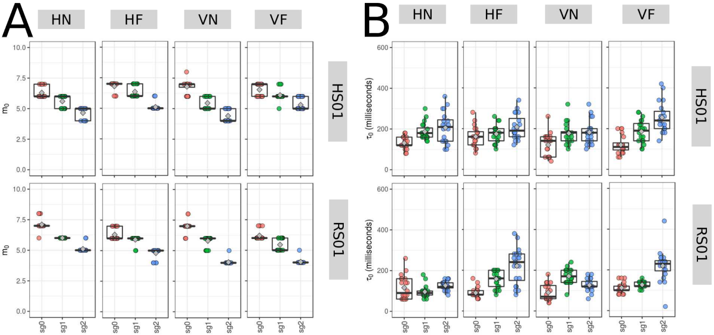

Figure 16: (A) Minimum Embedding Dimension (B) First Minimum AMI

Reconstructed State Spaces

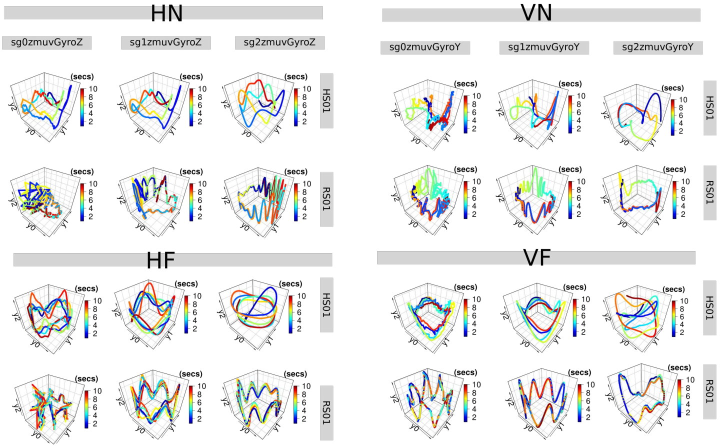

Figure 17: RSS for participant 01 computed with $(m = 6, \tau = 8)$ for different activities, signals and source of time-series data.

Recurrence Plots

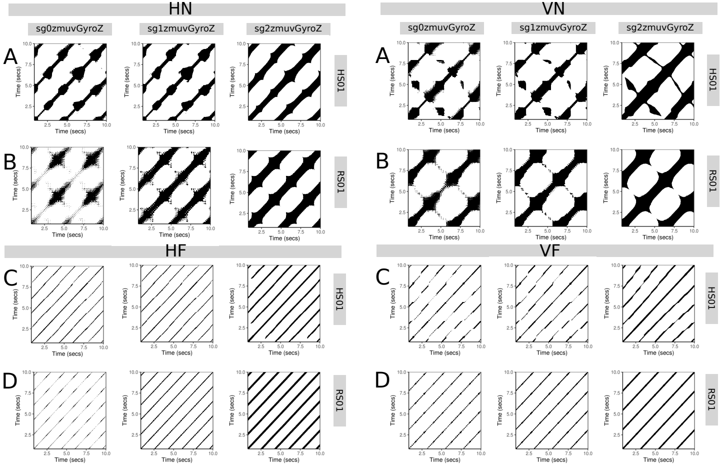

Figure 18: RP for participant 01 computed with $(m = 6,\ \tau = 8,\ \epsilon = 1)$ for different activities, signals and source of time-series data.

Recurrence Quantification Analysis

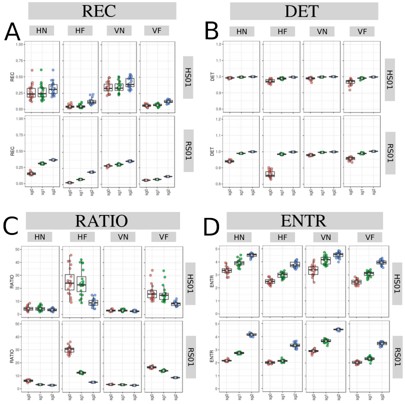

Figure 19: Box values of RQA computed with $(m = 7, \tau = 5, \epsilon = 1)$. These values are for 20 participants.

(Xochicale 2019 in **PhD Thesis**)

3D surfaces plots of RQA

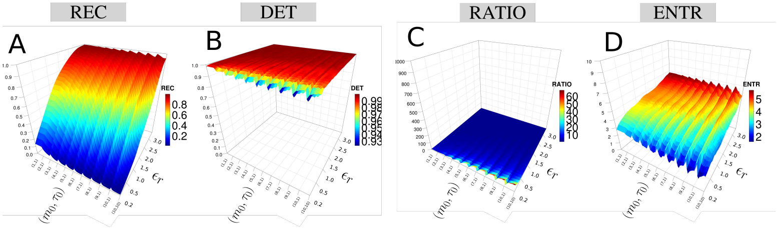

Figure 20: 3D RQA surfaces with increasing pair of embedding parameters $(0 \leq m \leq 10,\ 0 \leq \tau \leq 10)$ and recurrence thresholds $(0.2 \leq \epsilon \leq 3)$.

Sensors and activities

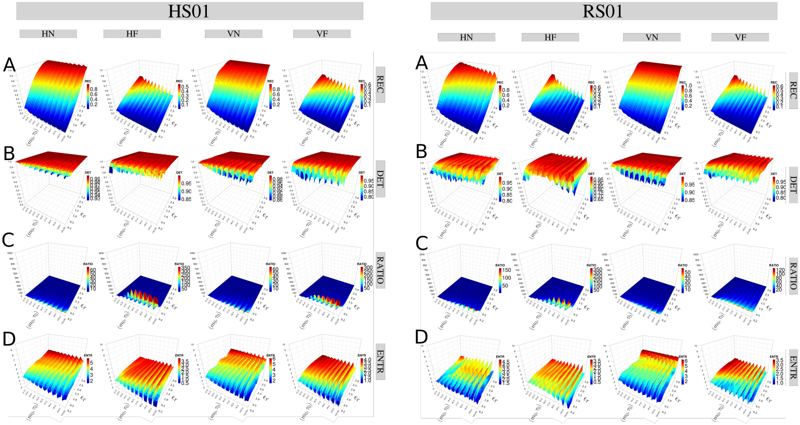

Figure 21: 3D surface plots of RQA for different sensors and activities.

Window size lengths

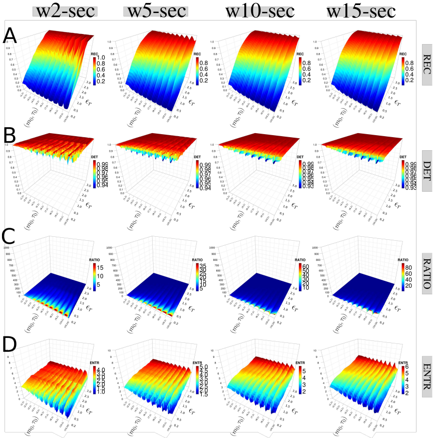

Figure 22: Window length size effect on 3D surface plots of RQA.

Smoothness

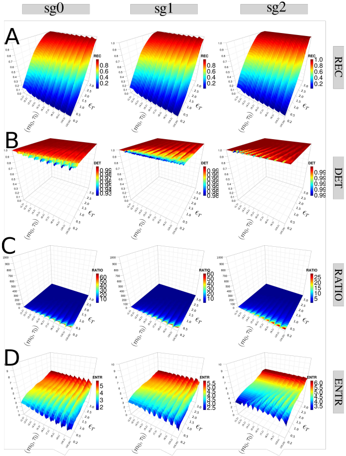

Figure 23: Smoothness effect on 3D surface plots of RQA.

Participants

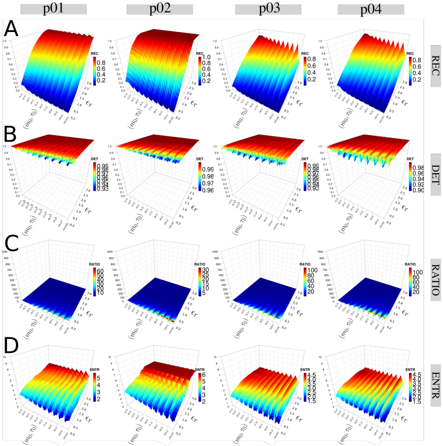

Figure 24: Participants differences of 3D surface plots of RQA.

(Xochicale 2019 in **PhD Thesis**)

CONCLUSIONS

Research Questions

- **Q1: What are the effects on RSSs, RPs, and RQA metrics of different embedding parameters, different recurrence thresholds and different characteristics of time series (structure, smoothness and window length size)?**
  The impact on nonlinear analysis tools is evidently for different data time-series. That said, the main contribution of this thesis is finding that measurements of entropy using 3D plot surfaces of RQA appear to be robust to real-word data (i.e. different time series structures, window length size and levels of smoothness).

Research Questions

- **Q2: What are the weaknesses and strengths of RQA metrics when quantifying movement variability?**
  WEAKNESSES: (i) requirement of an expert for interpretation and computation of nonlinear analysis results, (ii) laborious implementation, and (iii) nonlinear analysis does not give the best representation of the dynamics of time-series data.
  STRENGTHS: (i) little setup of parameters for 3D plot surfaces, and (ii) 3D plot surfaces can provide insight into the understanding of the dynamics of time-series data.

Research Questions

- **Q3: How does the smoothing of raw time series affect methods of nonlinear analysis when quantifying movement variability?**
  Smoothing raw time series can create well defined trajectories or patterns in RSS or RP, however such increase of smoothness can also create more complex (i.e. not well defined) trajectories or patterns in nonlinear analysis.

Applications of Nonlinear Dynamics

Quantification of skill learning

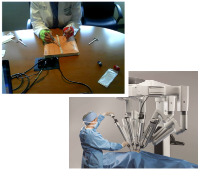

* Surgical Skills Assessment
* Robot-Assisted Surgery

Fetal behavioral development

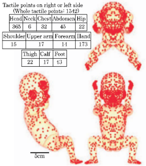

* General movements
* Arm/Legs Movs
* Hand/Face Contacts

Nonlinear Biomedical Signal Processing

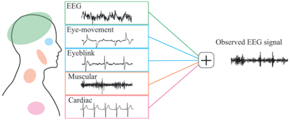

* EEG time series
* Heart rate variability
* Eye Movements

Future Work

Investigate

- other derivatives of acceleration data to have better understanding of the nature of human movement,
- other methodologies for state space reconstruction,
- the robustness of Entropy measurements with RQA, and
- variability in perception of velocity.

Considering context of human-humanoid interaction, the proposed method can be applied to

- evaluate improvement of movement performance,
- provide feedback of level of skillfulness, and
- quantify motor control problems and pathologies.

(Xochicale 2019 in **PhD thesis**)

OA Publications

PEER-REVIEW CONFERENCE PAPERS

- *Towards the Analysis of Movement Variability in Human-Humanoid Imitation Activities* (HAI2017)
- *Towards the Quantification of Human-Robot Imitation Using Wearable Inertial Sensors* (HRI2017)
- *Analysis of the Movement Variability in Dance Activities using Wearable Sensors* (WeRob2016)
- *Understanding Movement Variability of Simplistic Gestures Using an Inertial Sensor* (PerDis2016)

PREPRINTS & in preparation

- *Strengths and weaknesses of Recurrence Quantification Analysis in the context of human-humanoid interaction* (ArXiv, October 2018) for Scientific Reports.
- *3D surface plots of RQA Shannon Entropy*
  for Frontiers in Applied Mathematics and Statistics.

TALKS

- *Quantifying the Inherent Chaos of Human Movement Variability*
  15th Experimental Chaos and Complexity Conference
- *Towards the Analysis of Movement Variability for Facial Expressions with Nonlinear Dynamics*
  The 7th Consortium of European Research on Emotion Conference

FIRST Open Access PhD Thesis at UoB (since 1900)

https://github.com/mxochicale-phd/thesis

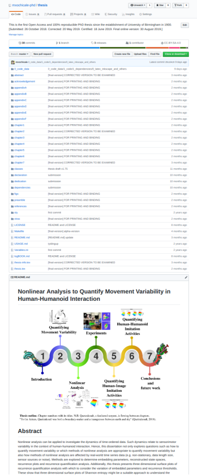

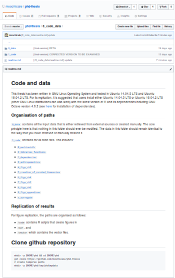

OA PhD Thesis

* LaTeX project

* Vector files

OA DATA

* Multidimensional Times-series
22 participants,
4 IMUs (6 axis), and
4 Activities.

OA SOFTWARE

* R version 3.4.4 (2018-03-15)

* R packages:
data.table
ggplot2
tseriesChaos
nonlinearTseries
RccArmadillo

* GNU Octave 4.0.2

(Xochicale 2019 in **PhD thesis**)

References

Xochicale Miguel
» Nonlinear Analysis to Quantify Movement Variability in Human-Humanoid Interaction «
Open Access Ph.D. Thesis (2019)
https://github.com/mxochicale-phd/thesis